International Journal of Multidisciplinary Research and Development
Online ISSN: 2349-4182, Print ISSN: 2349-5979, Impact Factor: RJIF 5.72
www.allsubjectjournal.com
Volume 4; Issue 2; February 2017; Page No. 01-11

Integrated approach of field and geophysical methods for the investigations of subsurface geology and potential sites for the artificial groundwater recharge in the NW part of Jordan

[*1] Mohammad Tarawneh, [2] MR Janardhana

[1] DOS in Earth Science, University of Mysore, Manasagangotri, Mysuru, Karnataka, India
[2] Department of Geology, Yuvaraja's College, University of Mysore, Mysuru, Karnataka, India

Abstract
In arid and semi-arid regions paucity of surface water resources exerts a great demand for groundwater. Successful application of artificial recharge method to augment the demand for groundwater warrants both direct and indirect approaches in the identification of potential sites for artificial groundwater recharge. The present study involving field studies, core log data, remote sensing technique and electrical resistivity soundings was carried out at the northwestern part of Jordan to identify suitable storage sites for the artificial recharge of the water bearing formations. A suitable storage site offers a great scope to meet the demand of water during the lean periods. Forty-three Vertical Electrical Soundings (VES) using the Schlumberger configuration of electrode array to map the subsurface geology have been conducted with maximum current electrode separations of 600 m. Distribution of the resistivity values at different depths are represented by iso-resistivity and electrical profile maps for different electrode spacing. Correlation of the obtained resistivity values with the geology of the area showed that five to six layers with varying hydrological properties exist in the study area. The study area was divided into three zones based on the feasibility for artificial recharge of groundwater; 'Most Suitable', 'Fairly Suitable ' and 'Less Suitable'. The southern and southeastern parts of the study area are identified as 'Most Suitable' area for the artificial recharge of groundwater as the area is characterized by a huge thickness of alluvium deposits. Water table in this part of the study area is found at greater depths thus signifying its capacity to receive high amounts of recharge water for storage. 'Fairly Suitable' area for groundwater artificial recharge is the northern part of the study area as it has medium to large thickness of alluvium deposits and water table at moderate depths. The central part of the study area is 'Less Suitable' for artificial recharge of the aquifer as water table is found at shallow depths although the thickness of the alluvium deposit is significant.

Keywords: DST, VES, iso-resistivity map, artificial recharge, Jordan valley, schlumberger electrode array

1. Introduction
Jordan is considered among the poorest countries in the world in terms of water resources. The high rate of population growth, the arid climate, the low and variable precipitation rates, the limited supplies, and over-exploitation of groundwater are all factors which rendered the problem more critical and dangerous. About 81% of its area receives rainfall in average less than 100 mm/year [1] and most of the received precipitation is being lost due to the high evaporation rates [2]. The annual population growth rate in Jordan is estimated to be around 2.7%. Based on this percentage, it is estimated that the total population in Jordan will be around 12 million by 2020 [3]. This will add more pressure on the existing meager water resources in the Jordan. During the year 2000, the per capita water share in Jordan was 234 cubic meter per annum and it is expected to be 111 cubic meter in the year 2020. This will place Jordan within the bottom 20% of the water poverty scale [4]. Intensive agricultural activities in some parts of Jordan Valley have during the last few decades led to extensive exploitation of groundwater resources. During the summer season, most of the eastern streams dry up and capturing the winter-flood water is one of the most critical aspects of water resources management in the Jordan Valley. Failure to store winter flood water or diverting it in a suitable way will lead to precious fresh water to flow directly to the Jordan river and then to the Dead Sea.

Artificial recharge of groundwater is used as an effective technique to fill aquifers using conventional and non-conventional water resources such as treated sewage effluents and excess storm water. This technique when applied properly allows the storage of stream flood water in the groundwater reservoirs and can be used during water crisis time for various purposes. Identification of the sites for the artificial recharge of aquifer calls for thorough understanding of the local geology and the subsurface structure. Numerous approaches are in practice for the purpose. However, field studies coupled with the applications of geophysical methods yield more promising results. Electrical resistivity method among various geophysical methods is used for a number of applications [5, 6, 7], particularly in the identification of groundwater potential zones [8, 9, 10, 11, 12, 13].

In the present study, field investigations including core logging, application of remote sensing technique and geoelectrical resistivity surveys were carried out with the aim of studying the suitability of a site in the area between Suleikhat and Yarmouk River for artificial groundwater recharge purpose. Attempts have also been made to correlate alluvial fans with feeding wadis (channels) as well as to correlate them with the Dead Sea Transform fault.

1.1 Study area
The study region is located in the north-western part of the Jordan (northern part of lower Jordan Valley). The study area lies between 32^0 41' and $32^0$18' N latitude; 35^0 42' and 35^0

33' E longitude as shown in Figure 1 covering an area of 504.3 Km^2. Topographically, the elevation of the land features ranges from 328 m below mean sea level to 860 m above mean sea level. It is bordered on both sides; east and west by high steep escarpments with differences in elevations between the valley floor and the surrounding mountains rising from 1200 m going up to 1700 m. Mounds of huge alluvial deposits occur throughout the study area (Fig. 2). The general slope in the study area decreases from east to west, varying from 30^0 to almost a 0^0. Many wadies (channels) such as Wadi Al Arab, Wadi Abu Al Ghoul, Wadi Al Tayyiba, Wadi Ziglab, Wadi Al Jurm, Wadi Al Hamam, Wadi Al Qarn and Wadi al Yabis run through the area. The distribution of rainfall varies from 200 mm/yr to 500 mm/yr. The higher elevated places get higher rainfall while lower elevation gets least rainfall. The soil characteristics of the terrain are the most important aspect, since it plays a major role in groundwater recharge. All the major textural types of soil are found in the study area. Various types of soil occur supporting gravels and pebbles in the region (Figs. 3 and 4).

The study area is a part of the Jordan valley basin with a sedimentary fill. The lithostratigraphic sequence of the study area [14] consists from bottom upwards (1) limestone, bedded massive dolomitic limestone and Dolomitic with chert beds, chalk limestone and marl of Cretaceous (Turonian-Maestrichtian) age, (2) chalk marls, marly limestone and chalky limestone of Paleocene-Miocene, (3) conglomerates, sands, silts and clayey marls of Pleistocene followed by (4) Holocene and Recent sediments including soil, calcrete, gravel, fluvial sediments and alluvial fan deposits. Recent sediment in the highland part of the study area is the lime crust (Calcrete) developed as over the carbonate rich clay and marl during the high seasonal rainfall. In the northern central part Upper Tertiary and Quaternary basalts cover the area.

The dominant structural feature in Jordan is the north-south trending Dead Sea Rift. The Dead Sea Transform fault (DST) is one of the major and most important structural and geological features in the world. It extends from Aqaba Gulf in the south to Taurus Mountains in the north with a length of 1100 km and a varying width of 5 to 20 km and it is a part of the east African-Syrian rift system of around 6000 km length from Turkey in the north to Ethiopia in the south [15]. The main structure in the study area is N-S trending sinistral strike-slip fault (Dead Sea Transform fault) in addition to E-W, ENE-WSW and ESE-WNW trending dextral strike-slip faults. Other secondary structures reported from the study area are the NW-SE trending tensional faults and NE-SW trending compression faults [16, 17].

Groundwater in the study area is mainly found in the Quaternary alluvial deposits composed of friable sediments which were brought in from the surrounding mountains. The hydrogeological classification of the study area is affected by the geological properties of the rock units. Salameh and Bannayan, 1993, classified the aquifer systems in the study area into three main aquifer complexes:

1- Deep sandstone aquifer complex.
2- Upper Cretaceous aquifer complex.
3- Shallow aquifer complex.

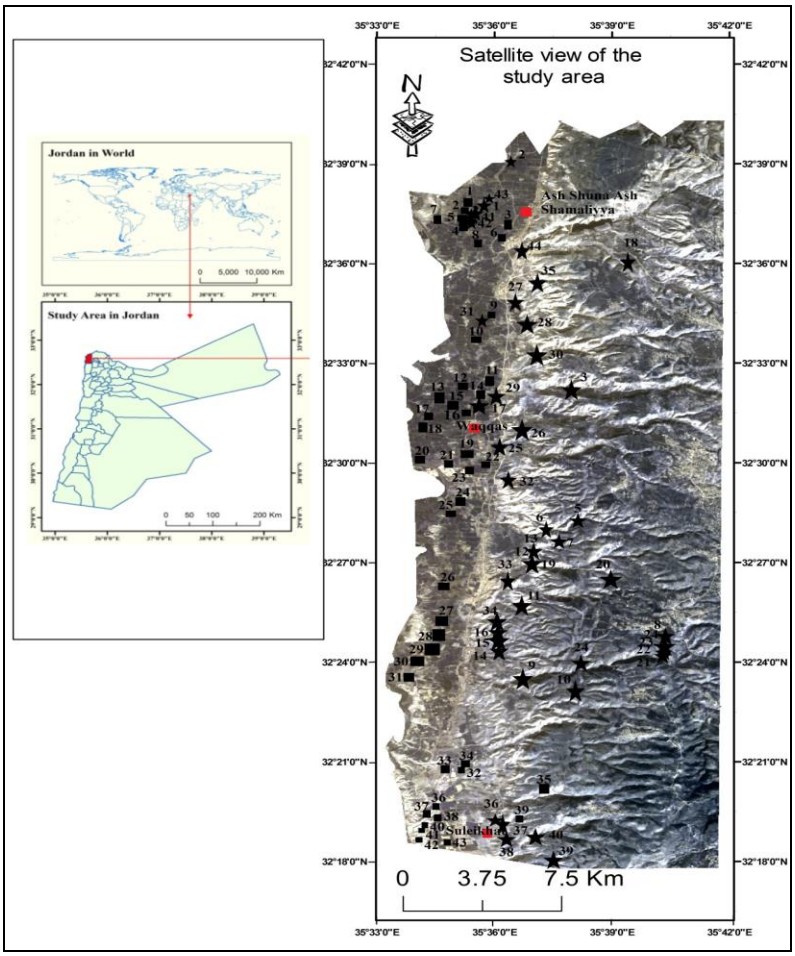

Fig 1: Location map of the study showing VES (■) and borehole stations (★).

2. Materials and methods

The study area contains many ancient and recent alluvial fans of varying size. Older alluvial fans exposed to weathering, erosion and human activities are not easily recognizable by field geologic mapping and the well logging methods. In order to supplement the well logging and other field data, indirect methods such as geophysical survey and remote sensing techniques are necessary.

The present field study was carried out based on the geological maps on a 1:250000 scale [18]. The study area was divided into several blocks and the locations of ancient and recent alluvial sediments were documented with GPS. Detection and documentation of the ancient and recent alluvial sediments in the study area as well as delineation of thematic layers such as land-use, lithology, lineament and soil types were aided by remote sensing technique also. For this purpose, satellite images (Landsat 8 OLI) were downloaded from USGS website (date of acquisition 3rd February 2016, swath 185km, ground resolution 30m, path 174 and row 38). After the collection of necessary satellite image data, the geometric, radiometric, atmospheric corrections have been performed by using ENVI software program. By using the GIS program and based on the WGS-1984 geographical co-ordinate system and UTM Zone 36 projection co-ordinate system, the images have been analyzed. In addition, core log and geophysical data were used to map alluvial fan deposits.

The drilling of boreholes was executed with a contract with Ministry of Water and Irrigation [19]. The drilling took place using a KSK rotary rig. Results were documented using ArcGIS10, Corel Draw, Rock Work 14 and IPI2win softwares. The geoelectrical resistivity method is one of the most effective geophysical methods for investigating the presence of groundwater and for groundwater potential sites [20, 21]. Electrical resistivity of soil and rocks depend on many factors such as, temperature, permeability, compaction and age of the rock, mineral and chemical compositions, fluid content in pores, shape and size of grains, porosity of soil and rocks, salinity and degree of saturation with water [22]. One of the most wide spread DC resistivity method is Vertical Electrical Sounding (VES) [23, 24]. Using Schlumberger configuration, VES at fourty three locations (Figure 1) were carried out by Campus Geopulse Resistivity meter. The maximum current electrodes separation extends to 600 m. The selection of soundings location was governed by the site conditions. The field measurements were processed and interpreted by IPI2win [25] software program.

The forty three vertical electrical sounding stations are distributed from north to south in the study area as shown in Figure 1. A few interpreted geoelectrical models for VES soundings are presented in Table 1, while Figures 5, 6 and 7 show three examples of layering model of VES curves.

The apparent resistivity values were obtained by multiplying the field resistance measurements by configuration factor at each of electrodes separation. The calculated apparent resistivity measurements were plotted against half of the current electrode spacing (AB/2) on bi-logarithmic scale. Traditional interpretation techniques such as curve matching and drawing auxiliary point diagram were applied. Based on these preliminary interpretations, an initial estimation of resistivities and thicknesses of various geoelectrical layers was obtained. These preliminary estimations were later used as a start model incorporating known geology and the available well data for a fast computer assisted interpretation IPI2win [25]. The field measurements were processed and interpreted by IPI2win [25] software program. Isoresistivity maps at various electrodes distances were constructed by using Rockwork14 software program. They were interpreted in terms of resistivities and thicknesses of various subsurface layers.

Fig 2: Field photograph showing alluvial fan deposit in Suleikhat area (32° 19' 52" N 35° 36' 57" E).

Fig 3: Gravels and pebbles set in the marl rich matrix in the alluvial fan deposits in the study area (Northeast Ash Shuna)(32° 38' 17" N 35° 39'28 " E).

Fig 4: Mud matrix supported clasts in the study area (Waqqas area) (32° 34' 17" N 35° 37'28 " E).

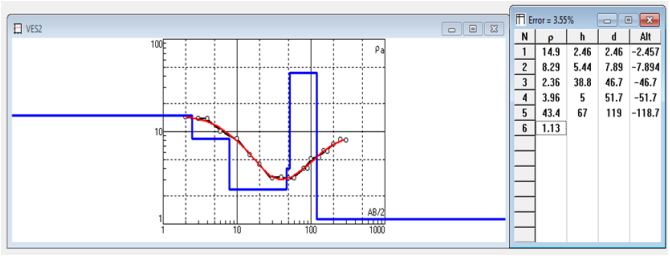

Fig 5: Modeling of a sounding point VES2: measured apparent resistivity (white dots), best-fit model (tabulated and as a graph in logarithmic scale) and related curve model (full line) are shown (North of study area).

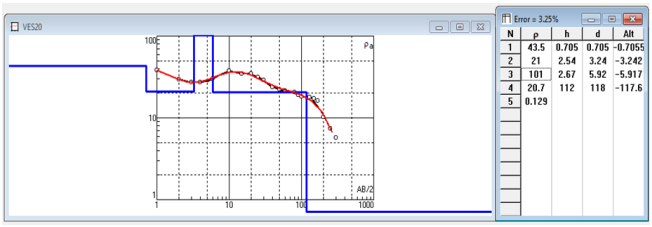

Fig 6: Modeling of a sounding point VES20: measured apparent resistivity (white dots), best-fit model (tabulated and as a graph in logarithmic scale) and related curve model (full line) are shown (Middle of study area).

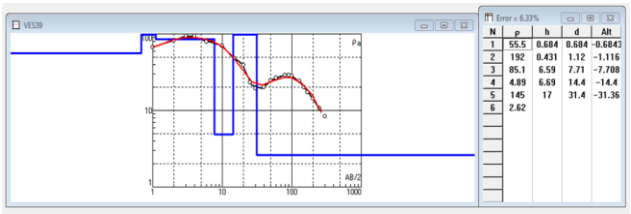

Fig 7: Modeling of a sounding point VES39: measured apparent resistivity (white dots), best-fit model (tabulated and as a graph in logarithmic scale) and related curve model (full line) are shown (South of study area).

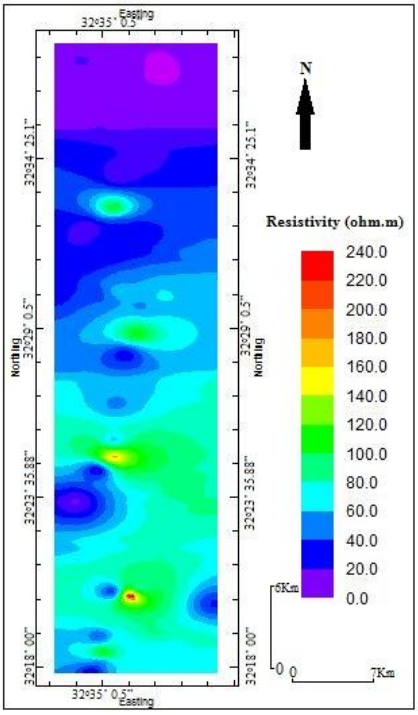

Fig 8: Iso-resistivity map at half electrodes separations (AB/2=2m).

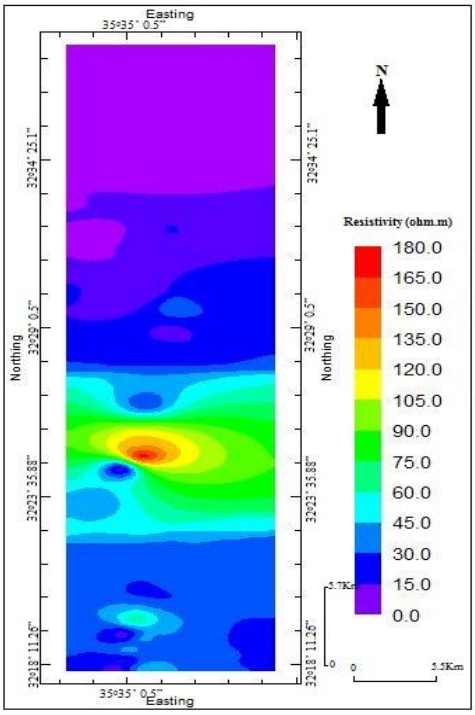

Fig 9: Iso-resistivity map at half electrodes separations (AB/2=50m).

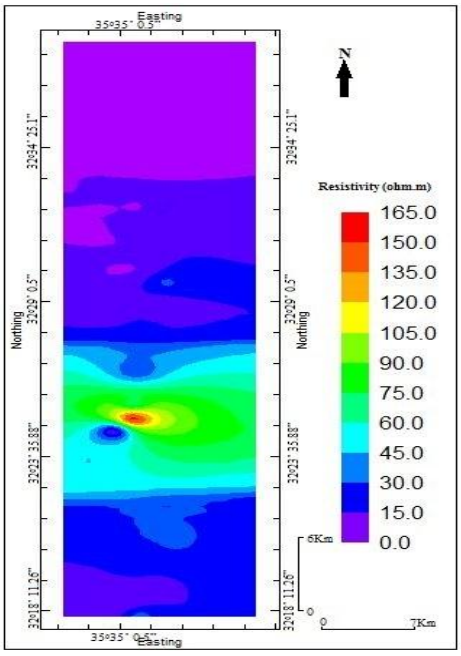

Fig 10: Iso-resistivity map at half electrodes separations (AB/2=100m).

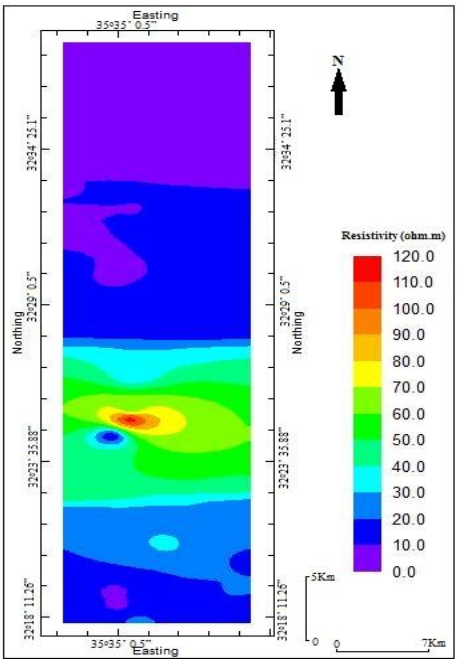

Fig 11: Iso-resistivity map at half electrodes separations (AB/2=150m).

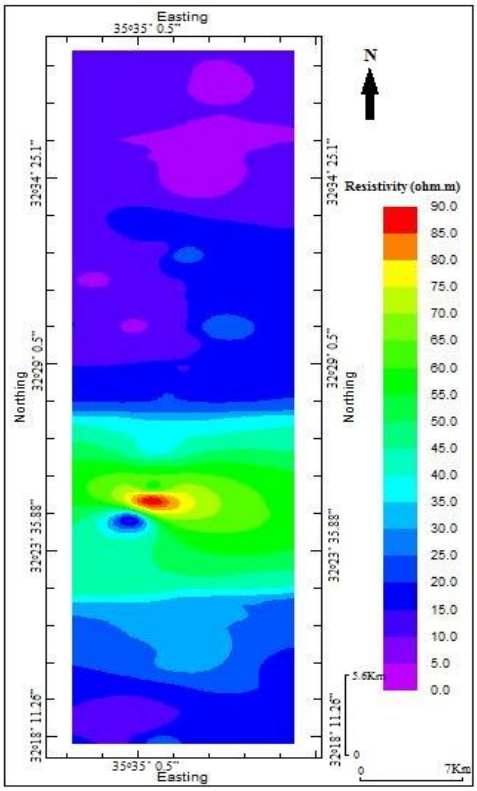

Fig 12: Iso-resistivity map at half electrodesseparations (AB/2=200m).

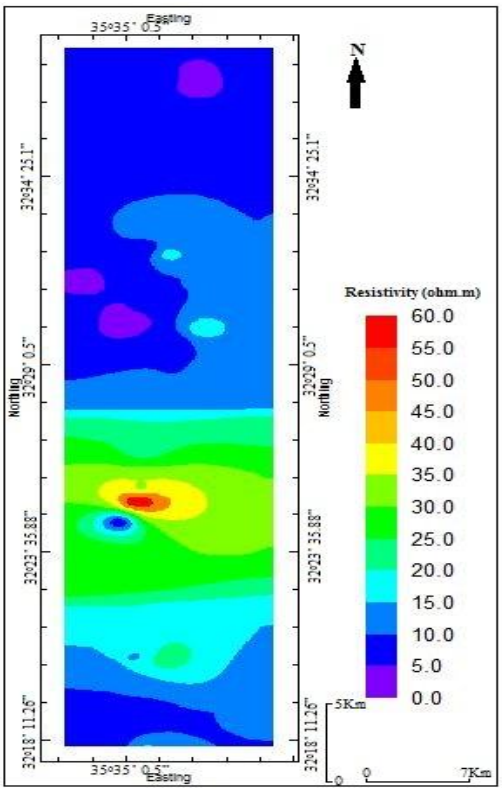

Fig 13: Iso-resistivity map at half electrodes separations (AB/2=250m).

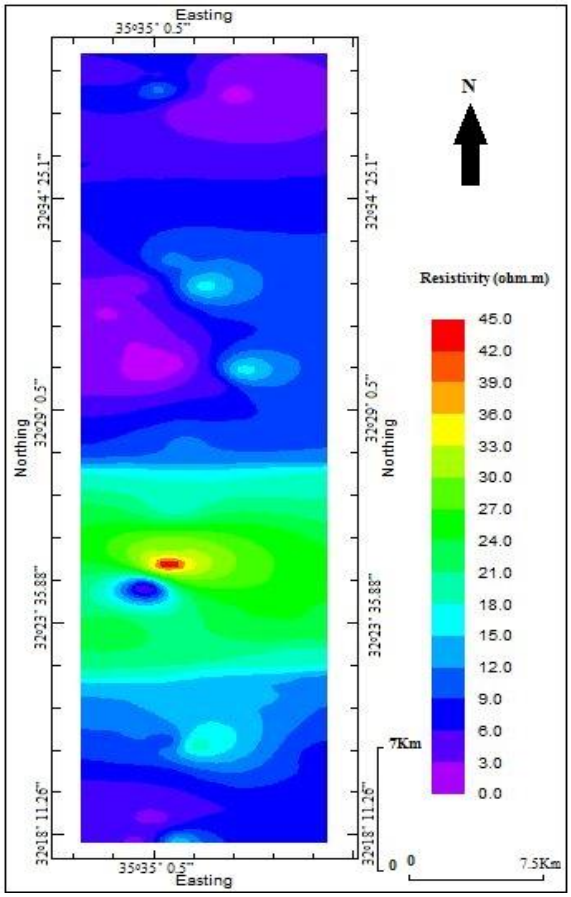

Fig 14: Iso-resistivity map at half electrodes separations (AB/2=300m).

Table 1: Interpretation of some multilayer best-fit model of VES's

VES. NO	Resistivity (Ohm m)	Depth (m)	Suggested lithological interpretation based on available surface geological and well log data
VES1	9.22	G.S* - 8.89	Wet top soil consisting mainly of silty clay and clay
	2.59	8.89 - 40.8	Marly clay
	79.6	40.8 - 83.3	Saturated alluvium sediments consisting mainly of limestone
	0.3	>83.3	Lisan marls formation or highly clay content or highly saline clay groundwater
VES2	14.9	G.S* - 2.46	Wet top soil consisting of silty clay and clay
	8.29	2.46 – 7.89	Wet top soil consisting of silty clay and clay
	2.36	7.89 – 46.7	Marly clay
	3.96	46.7 – 51.7	Marly clays
	43.4	51.7 – 119	Saturated alluvium sediments consisting mainly of limestone.
	1.13	>119	Marl of lisan marl formation or highly clay content or a saline clay groundwater
VES3	8.46	G.S* - 2.79	Highly clay content top soil
	4.15	2.79 – 8.58	Saline groundwater interbedded with clay
	2.86	8.58 – 23.1	Saline groundwater interbedded with clay
	13.8	23.1 – 47.9	Saturated alluvium sediments consists mainly of silty clay and clay
	3.12	>47.9	Lisan marl formation or highly clay content or a saline clay groundwater
VES16	22.3	G.S* - 0.66	Wet top soil
	48.7	0.66 – 1	Saturated alluvium sediments consists mainly of gravel of limestone
	174	1 – 2.46	Unsaturated alluvium sediments consisting of gravel of limestone and dolomitic limestone
	13	2.46 – 25.6	Saturated alluvium deposits consisting mainly of silty clay and clay
	39	25.6 – 51.7	Saturated alluvium deposit
	5.92	>51.7	Lisan marls formation or highly clay content
VES20	43.5	G.S* - 0.71	Dry top soil
	21	0.71 – 3.24	Saturated alluvium sediments consists mainly of silty clay and clay
	101	3.24 – 5.92	Unsaturated alluvium deposits consists mainly of gravel of limestone and dolomitic limestone
	20.7	5.92 – 118	Alluvium sediments consisting mainly of silty clay and clay.
	0.129	>118	Lisan marls formation or highly clay content.
VES25	32.3	G.S* - 2.52	Dry top soil
	7.24	2.52 – 4.67	Silty clay and clay
	132	4.67 – 8.93	Unsaturated alluvium sediments consists mainly of gravel of limestone and dolomitic limestone
	21.5	8.93 – 96.2	Saturated alluvium sediments consisting mainly of silty clay and clay
	8.24	>96.2	Saline clayey or lisan marl formation.
	12.6	>75.9	Saturated alluvium sediments consists mainly of silty clay and clay
	8.72	>35.9	Lisan marl formation or a highly content of clay
VES32	85.4	G.S* - 1.78	Saturated alluvium sediments consists mainly of limestone
	14.1	1.78 – 9.83	Saturated alluvium sediments
	36.1	9.83 – 18.2	Saturated alluvium sediments
	107	18.2 – 47.5	Unsaturated alluvium sediments consists mainly of limestone and dolomitic limestone
	10.9	>47.5	Saturated alluvium sediments with highly content of clay
	33.1	3.63 – 7.23	Saturated alluvium layer
	6.86	7.23 – 14.1	Clay
VES37	13.4	G.S* - 0.28	Wet top soil
	55.8	0.28 – 3.94	Saturated alluvium sediments
	3.62	3.94 – 36	Clay or marly clay
	35.3	36 – 73.8	Saturated alluvium sediments
	0.144	>73.8	Highly clay content of lisan marl formation
VES39	55.5	G.S* - 0.68	Dry top soil
	192	0.68 – 1.12	Alluvium sediments consisting mainly of gravel of limestone and dolomitic limestone
	85.1	1.12 – 7.71	Saturated alluvium sediments
	4.89	7.71 – 14.4	Marly clay
	145	14.4 – 31.4	Unsaturated alluvium sediments consists mainly of coarse grain of limestone and dolomitic limestone
	2.62	>31.4	Highly clay content of lisan marl formation or a saline clay groundwater

G.S*: Ground Surface

3. Results & Discussion

3.1 Field and remote sensing work

The study area contains many ancient and recent alluvial fans of varying size. Ancient alluvial fans are confined to the western part of the study area (Figure 15). The older alluviums have been exposed to weathering, erosion and human activities (agriculture and building) and by field geologic mapping cannot be recognized. Thick sequences of alluvial sediments with distinct internal stratification cover the intersection of valley and the western side of the Dead Sea fault. The sediments are very coarse grained, consisting of angular to sub-rounded clasts indicating them to be of proximal origin of the alluvial fan deposits. Debris flow deposits are also noticed at some places which are characterized by very poorly sorted sediments, massive with either marl or mud matrix supported clasts. These sediments are known to have high to very high water yielding potential. Table 2 shows the vertical stratification of the ancient and

recent alluvial fans and gives a general geological picture along north, middle and south parts of the study.

Displacement of alluvial deposits owing to the strike shift fault along the foot hills of the Jordan Rift Valley in the study area is commonly noticed. This has resulted in the separation of the alluvial fan deposits from their feeding wadis. To cite a few examples, alluvial fan deposits of Suleikhat area located in the southern part of the study area have been displaced in the northern direction by more than 500 m from its source. The alluvial fan deposits of Wadi Al Qarn have been shifted by about 2000 m in the northern direction from its feeding wadi.

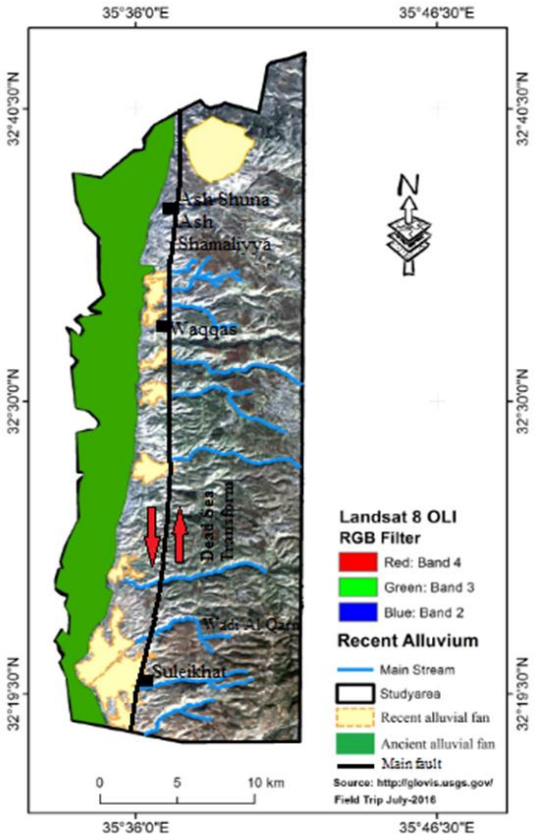

Fig. 15: Location map of the ancient and recent alluvial sediments.

Table 2: Vertical stratification of the ancient and recent alluvial fans in the study area.

North	Middle	South	Thickness
Soil	Soil	Soil	Few centimeters to few meters
Alluvium sediments consists mainly of gravels, highly clay content, marly clay and silty clay	Alluvium sediments consists mainly of gravels of limestone, dolomitic limestone, marly clay and silty clay	Alluvium sediments consists mainly of coarse grain of gravels of limestone, chert, dolomitic limestone, marly clay and silty clay	>1m
Increasing in clay content	Increasing in clay content	Increasing in clay content	>1m

3.2 Geoelectric survey

For better understanding of the subsurface geology of the study area, modeling of VES curves were carried out. Three VES curves representing north, central and southern parts of the study area are considered here for discussion. Results of the selected geoelectric survey have been shown in Figures 5, 6 and 7. Interpretation of the VES curves have been carried out based on the field data as well as the obtained resistivity data. Figure 5 shows a six geoelectrical layers at VES2 station. The first and second layers are interpreted as a wet top soil consisting of silty clay and clay. The third and fourth layers are interpreted as a marly clay layers. The fifth layer resistivity is 43.4 ohm m and its thickness is 67 m, and is interpreted as saturated alluvium sediments consisting mainly of limestone. Beneath this layer the resistivity is 1.13 ohm m indicating to the marl of lisan marl formation or highly clay content or a saline clay groundwater. The layering model of VES20 is presented in Figure 6. It shows a five geoelectrical layers. The first layer resistivity is 43.5 ohm m with thickness of 0.705 m, and is interpreted as a dry top soil. The second layer resistivity is 21 ohm m with thickness of 2.54 m, and is interpreted as saturated alluvium sediments consists mainly of silty clay and clay. The third layer resistivity is 101 ohm m with thickness of 2.67 m and is interpreted as an unsaturated alluvium deposits consists mainly of gravel of limestone and dolomitic limestone. The fourth layer resistivity is 20.7 ohm m with thickness of 112 m, and is interpreted as saturated alluvium sediments consisting mainly of silty clay and clay. The last layer resistivity is 0.129 ohm m, and is attributed to lisan marls formation or highly clay content. The layering model of VES39 is presented in Figure 7. It shows a six geoelectrical layers. The first layer resistivity is 55.5 ohm m, and its

thickness is 0.684 m, and is interpreted as a dry top soil. The second layer resistivity is 192 ohm m and its thickness is 0.431 m, and is interpreted as unsaturated alluvium sediments consisting mainly of gravel of limestone and dolomitic limestone. The third layer resistivity is 85.1 ohm m and its thickness is 6.59 m, and is interpreted as a saturated alluvium sediments. The resistivity of the fourth layer is 4.89 ohm m with a thickness of 6.69 m, and is attributed to marly clay layer. The resistivity of the fifth layer is 145 ohm m with thickness of 17 m, and is interpreted as an unsaturated alluvium sediments consists mainly of coarse grain of limestone and dolomitic limestone. The resistivity of the last layer is 2.62 ohm m, and is interpreted as a highly clay content of lisan marl formation or a saline clay groundwater.

The iso-apparent resistivity maps at all separations show that the southern, southeastern and middle parts of the study area have a high values relative to the northern and northeastern parts. So this indicates the presence of alluvium sediments, dry sand, coarse grains gravel and refers to presence of fresh water at depths corresponding to these electrode separations. It is also shown that the most northern parts of the study area are characterized by a low resistivity zone. This can be attributed to the presence of the high clay, silty clay content and /or the salinity of the ground water in this area or indicates the presence of the saline clays of the lisan formation. Generally the spatial distribution of apparent resistivity measurements at different depths showed a general decrease in the measured resistivity in western and northern direction.

Of most importance in the qualitative interpretation of electrical resistivity data, is to classify the observed apparent resistivity curves into types [22]. This classification was primarily made on the basis of the shapes of the sounding curves, and it's relation to the geological situation in the subsurface. For example in Figure 5 the resistivity curve is classified as QHA because ($\rho1 > \rho2 > \rho3 < \rho4 < \rho5 > \rho6$). In Figure 6 the resistivity curve is classified as HKQ because ($\rho1 > \rho2 < \rho3 > \rho4 > \rho5$) and in Figure 7 the resistivity curve is classified as KQH because ($\rho1 < \rho2 > \rho3 > \rho4 < \rho5 > \rho6$).

Another useful and practical classification was made on the basis of the ranges of the observed resistivity measurements. By the analysis of the ranges of observed resistivity measurements it was possible to categorize the observed curves into three main classes. They are: (1) High resistivity class: this class belongs to an observed curve where most of the observed apparent resistivity readings recorded are greater than (80 ohm m), (2) Intermediates resistivity class: this class belongs to an observed resistivity curve where the most of the resistivity readings are within the range (30-80 ohm m) and (3) Low resistivity class: this class belongs to observed resistivity curves where most of observed resistivity readings is less than 30 ohm m. In the study area, High resistivity type reflects the presence of huge thickness of alluvium deposits consisting mainly of coarse grain, boulders, gravels and sands deposits. The sounding points of High resistivity type are concentrated in the eastern and southern parts of the study area and on the alluvial fans deposits. The resistivity values in the range of Intermediate resistivity type reflect the presence of alluvium deposits consisting mainly of sand, silt, and low amounts of clays, and groundwater of intermediates salinity. The sounding points of this type are concentrated in the middle part of the alluvium deposits in the study area. Low resistivity type resistivity values are correlated to the presence of clayey sediments with the presence of saline groundwater. They occur in the northern parts of the study area. Most of VES stations in the northern parts of the study area recorded resistivity values less than 30 ohm m, the middle part between 30-80 ohm m and the southern part more than 80 ohm m.

From the iso-resistivity maps and observed resistivity curves, the values of the apparent resistivity in most VES stations decrease to a about 1-20 ohm m with the increase in the current electrode separations, indicating a conductive substratum layer, this resistivity is referred to the clay content of lisan formation and or the salinity of clay and or the salinity of the ground water in this area.

Figure 16 shows geoelectrical cross section along sounding points VES7 and VES6, this cross-section oriented in a NW-SE direction with distance about 3.1 km. Sounding point VES7 resistivity characterized as intermediate to high and the sounding point VES6 resistivity characterized as low to intermediate. The resistivity decreases from NW to SE in this section. Figure 17 shows geoelectrical cross section along sounding pointsVES20, VES21 and VES22, this cross-section oriented in a E-W direction with distance about 3.1 km. Sounding point VES20 resistivity characterized as low to intermediate, sounding point VES21 resistivity characterized as low to high and sounding point VES22 resistivity characterized as intermediate to high. The resistivity increases from W to E in this section. Figure 18 shows geoelectrical cross section along sounding pointsVES26, VES27, VES28, VES29 and VES37, this cross-section oriented in a NNE-SSW direction with distance about 12.9 km. The resistivity increases from NEE to SSW but at the end of the section (VES37) decrease. Figure 19 shows geoelectrical cross section along sounding pointsVES42 and VES39, this cross-section oriented in a NE-SW direction with distance about 5.1 km. The resistivity under sounding point VES42 characterized as low to intermediate resistivity and under sounding point VES39 characterized as low to high resistivity. The resistivity increases from SW to NE. Figure 20 shows geoelectrical cross section along sounding pointsVES43, VES33, VES28, VES26, VES25, VES19, VES12, VES10 and VES8, this cross-section oriented in a N-S direction with distance about 32.35 km. The resistivity increases from N to S.

From the iso-resistivity maps, observed resistivity curves and geoelectrical cross sections we can deduce the resistivity in the study area increase from northern parts to southern parts and also increase from western to eastern parts of the study area. Which mean the most of southern and eastern parts have a large thicknesses of alluvium sediments consists mainly of coarse grain, boulders, gravels and sands deposits with low amount of clay content, where the most of western and northern parts of study area have alluvium sediments consists mainly of highly clay, marly clay and silty clay content.

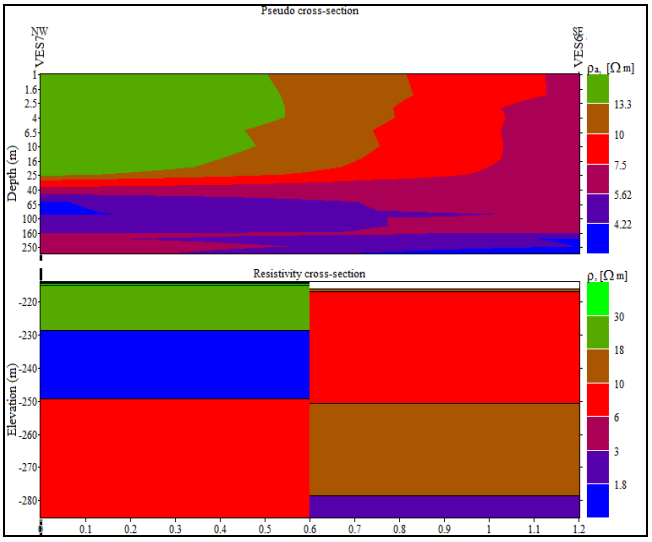

Fig. 16 Interpreted pseudo cross-section and true resistivity cross-section along sounding points VES7 and VES6, with depths between 0 to 250 (mbgs).

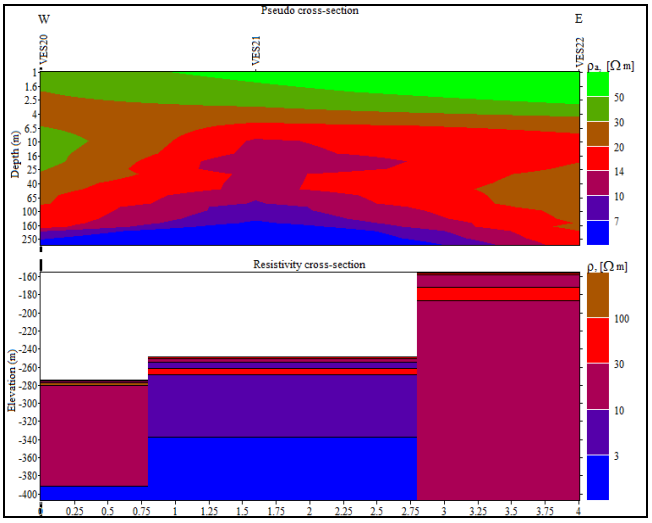

Fig. 17 Interpreted pseudo cross-section and true resistivity cross-section along sounding points VES20, VES21 and VES22, with depths between 0 to 250 (mbgs).

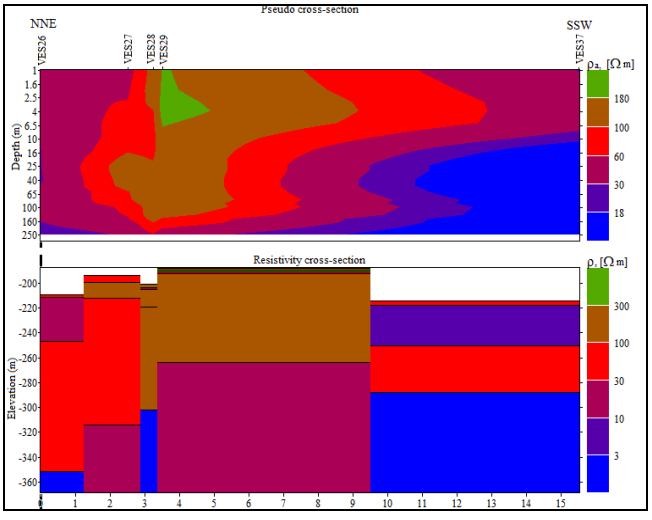

Fig 18: Interpreted pseudo cross-section and true resistivity cross-section along sounding points VES26, VES27, VES28, VES29 and VES37,with depths between 0 to 250 (mbgs).

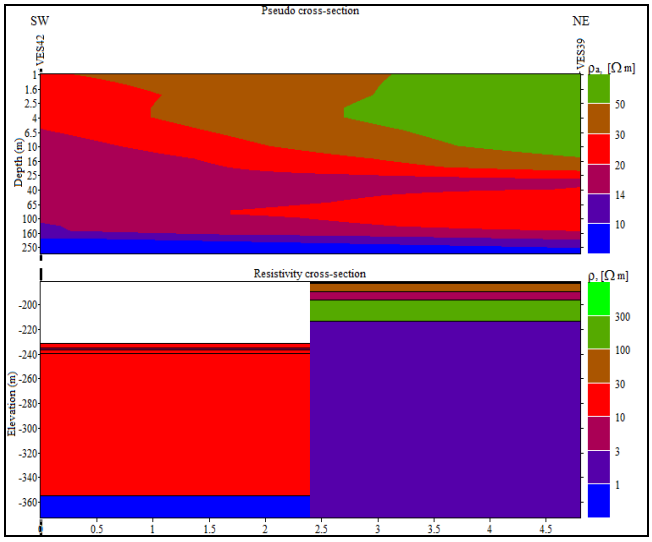

Fig 19: Interpreted pseudo cross-section and true resistivity cross-section along sounding points VES42 and VES39, with depths between 0 to 250 (mbgs).

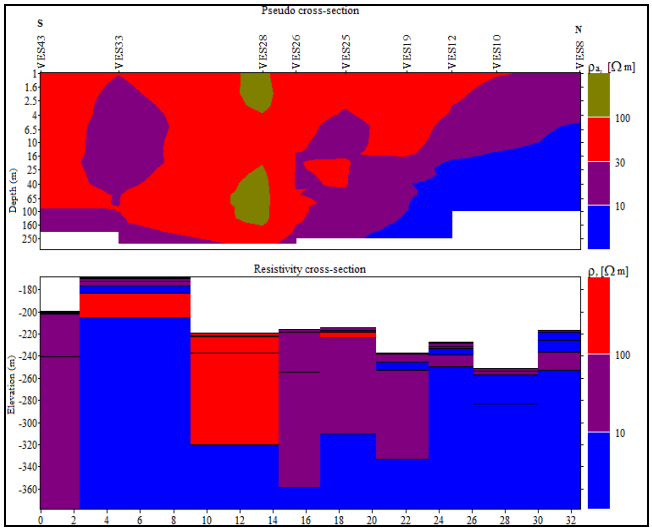

Fig 20: Interpreted pseudo cross-section and true resistivity cross-section along sounding points VES43, VES33, VES28, VES26, VES25, VES19, VES12, VES10 and VES8, with depths between 0 to 250 (mbgs).

3.3 Drilling activities in the study area

Identification of sites for recharge and storage of groundwater is greatly facilitated by the study of the hydrogeological and lithological set up of the study area. The purpose of drilling is to identify suitable sites that can help in the planning of artificial recharge projects and support and calibrate the results obtained from the Geo-electrical survey method. The locations of the boreholes and lithological description of each bore hole are shown in Figures 1 and 21 respectively. The locations of drilling were determined basically based on the results of geoelectrical survey measurements.

Southern part of the study area is covered with thick alluvium deposits consisting mainly of coarse grain, boulders, and gravels of limestone, chalky limestone, chert and dolomitic limestone. Middle parts of the study area have alluvium deposits consisting mainly of gravels of limestone with marl, silty clay and low amounts of clays. The alluvium sediments in the northern parts consist mainly of gravels with clay, marly clay, marl and silty clay.

3.4 Calibration model

The borehole logs information together with the geoelectric data and water level are found to fit into categories; first category, clay, silty clay, marly clay and clay with saline groundwater (<10 ohm m), second one, saturated alluvium consisting mainly of clay, silty clay and marly clay (10-30 ohm m), third one, saturated alluvium consisting mainly of fine grain of limestone (30-100 ohm m), fourth one, unsaturated alluvium consisting mainly of coarse grain of limestone and dolomitic limestone (>100 ohm m), fifth one, wet top soil consisting mainly of clay, silty clay and marly clay (10-30 ohm m) and the last one, dry top soil consisting mainly of limestone (30-60 ohm m). The interpretation of sounding data yielded true resistivity values which range from about 1 ohm m to more than 400 ohm m. The obtained range of true resistivity values correspond to clay or saline clay on the lower value side through dry sand, gravel, saturated and to unsaturated alluvium sediments at the high values of true resistivity.

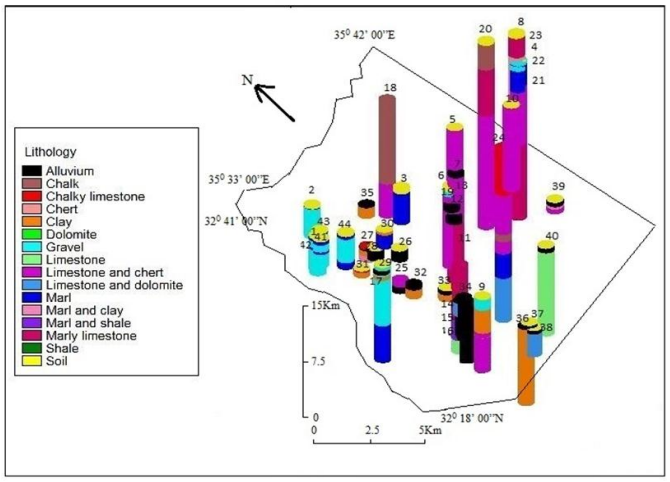

Fig 21: Constructed diagram to show lithologic log for boreholes in the study area (3D).

The alluvial sediment thickness or the depth to the Lisan Marl Formation (LMF) throughout the study area was estimated by examining each interpreted resistivity depth profile together with the borehole logs information, and selecting the depth at which resistivity values decreased to below 1-4 ohm.m. The depth of LMF represents the location of the contact between the alluvium and the underlying of lisan marl formation. In this interpretation is the assumption that the lisan marl formation has a much smaller resistivity value than the overlying saturated alluvium. So the study area can be classified based on the thickness of the alluvium deposits into three sub-zone, northern part of the study area (North Shuna area), where the thickness of alluvium deposits ranges from 40 m to 120 m, with an average of 63.2 m. Middle part of the study area (South Waqqas area), where the thickness of alluvium deposits ranges from 20 m to 150 m, with an average of 72.93 m, and the southern part of the study area (North Suleikhat area), where the thickness of alluvium deposits ranges from 10 m to 190 m, with an average of 78.6 m. In the study area, generally from 10 m to 190 m in the study area, with average of 73.36 m.

The unsaturated zone thickness or the depth to the water table was determined based on results of drilling activities, geoelectric sounding surveys together with the lithological information of available wells. The largest thickness of the unsaturated zone was found in the southern and southeastern parts of the study area (Suleikhat area), with ranged between 20 m to 220 m, and with an average of 68.88 m. The smallest thickness of the unsaturated zone was found in middle part of study area (Waqqas area), which ranged between 2 m to 80 m, and with an average of 14.69 m. While in the most northern part of the study area, the thickness of the unsaturated zone ranged from 20 m to 60 m, and with an average of 34.54 m. In the study area, generally the thickness of the unsaturated zone increases from west to east and from north to south.

4. Conclusions

Geologic structures in the study area seems to control, in addition, to topographic features, catchment area, drainage, sedimentation areas of alluvial deposits also the positions and situation of the alluvial deposits. The sinistral shift along the foot hills of the Jordan Rift Valley in the study area has resulted in alluvial fan deposits being separated from their feeding wadis to be found to the south of these wadis. As an example, the alluvial fan deposits of Suleikhat area (south part of study area) do not have at present to its east, north east or south east a wadi, which might have brought the huge amount of sediments (gravel and sand) accumulated there of about 1.5 km in N-S direction and 2 km in E-W direction and a depth of not less than 100 m. the next major feeding wadi lies at present at about 500 m from the northern end of the alluvial fan. This means that the feeding wadi (Wadi Al Qarn) lies at present at about 500 m from the northern end of the alluvial fan. This means that the feeding wadi (Wadi Al Qarn) has shifted to the north by about 2000 m (deposition of alluvial sediment must have started in the northern end of the alluvial fan).

The locations of buried and masked alluvial fans in the study area were defined using indirect geological and geophysical techniques such as, geoelectrical surveys (VES) and geologic correlations. These results of these techniques were verified by drilling of boreholes and correlations of well geologic logs. These buried alluvial fans must have feeding wadis, which due to the sinistral strike slip movement has migrated to the north along the strike slip fault. This further means by a slip rate of 4-6mm/yr [15, 28, 29, 30] an age of alluvial fan of ($333*10^3$) to ($500*10^3$) years. The result of locating buried alluvial fans, and correlating them to feeding wadis an additional proof of the strike slip movement and eventually the rate of movement, if the age of alluvial deposits can be determined.

From the field work, geoelectric survey and drilling boreholes data, southern parts of the study area have a high thickness of alluvium deposits consisting mainly of coarse grain, boulders, and gravels consist mainly of limestone, chalky limestone, chert and dolomitic limestone with low amount of clay content and it has a large thickness of unsaturated zone (water table). Middle parts of the study area have an alluvium deposits mainly consisting of gravels of limestone with marl, silty clay and low amounts of clays and it has shallow to medium thickness of unsaturated zone (water table). The alluvium sediments in the northern parts consist mainly of gravels with highly clay, marly clay, marl and silty clay contents and it has a large thickness of unsaturated zone (water table) and it has shallow to medium thickness of unsaturated zone (water table).

In term of suitability for artificial recharge of groundwater, the

study area can be divide into three zones; "Most Suitable" area for groundwater artificial recharge in southern (Suleikhat area) and southeastern parts of the study area (32° 18' 00" N to 32° 25' 00" N), because it characterized by a large thickness of alluvium deposits (10-190 m), with an average of 78.6 m, and it also have relatively a deep groundwater level (20-220 m), with an average of 68.88 m, which mean it capacity and ability to receive high amounts of recharge water for storage. Second zone is "Fairly Suitable" area for groundwater artificial recharge in northern part of the study area (Ash Shuna area) (32° 34' 00" N to 32° 41' 00" N), because it's characterized by a medium to large thickness of alluvium deposits (40-120 m), with an average of 63.2 m, and it has a shallow to medium groundwater level (20-60 m), with an average of 34.54 m. Third zone is "Less Suitable" area for groundwater artificial recharge (Waqqas area) (32° 25' 00" N to 32° 34' 00" N), because it characterized by shallow to medium groundwater level (2-80 m), with an average of 14.69 m, and medium to large thickness of alluvium deposits (20-150 m), with an average of 72.93 m.

5. References

1. Ministry of Water and Irrigation (MWI) Open Files, Jordan, 2011. www.mwi.gov.jo.
2. Salameh E, Bannayan H. Water Resources of Jordan. Present Status and Future potentials, Fridrich Ebert Stiftung, Amman, Jordan, 1993; 1:151-260.
3. UNPD. Sustaining Water: An Update World Population Prospects, the 1994 Revision. The United Nations, New York, In: M. Shahin, Ed., Water Resources and Hydro-meteorology of the Arab Region, Netherlands, 2007, 525-526.
4. Lawrence P, Meeigh J, Sullivan C. The Water Poverty Index: an International Comparison, 2002, (ISSN 1352-8955).
5. Nupearachchi CN, Prematilaka KM, Attanayake ANB, Fernando GWAR. Subsurface Geological and Hydrogeological Conditions of the Matale District, OUSL Journal Sri Lanka. 2010; 6:91-102.
6. Jinmin M, Saad R, Saidin M, Bery AA. Electrical resistivity survey in Bukit Bunuh, Malaysia for subsurface structure of meteorite impact study. Open Journ. Geol, V. 3, 34-37.
7. Bankole SA, Olasehinde PI, Ologe O, Ibrahim KO. Geological and Electrical Resistivity Sounding of Olokonla Area in North-Central Nigeria, Nigerian Journal of Technological Development. 2014; 11:12-16.
8. Sabale SM, Ghodake VR, Narayanpethkar AB. Electrical Resistivity Distribution Studies for artificial recharge of groundwater in the Dhubdhubi Basin, Solapur District, Maharashtra, India. J. Ind. Geophys. 2009; 13:201-207.
9. Muralitharan J, Palanivel K. GIS based lineament Delineation using geophysical resistivity data, Karur district, Tamil Nadu, India. Intnatl Jour Geomat and Geoscis, 2012; 3:167-177.
10. Coker JO. Vertical electrical sounding (VES) methods to delineate potential groundwater aquifers in Akobo area, Ibadan, South-western, Nigeria. Journal of Geology and Mining Research. 2012; 4:35-42.
11. Khan GD, Waheedullah, Bhatti AS. Groundwater Investigation by Using Resistivity Survey in Peshawar, Pakistan. Jour Res Dev Mangmt. 2013; 2:9-20.
12. Akawwi E, Al-Zoubi A, Abu-Aldes AR, Al-Rzouq R. Using vertical electrical sounding for locating static water level and geological features in Aqaba area, Jordan. Res. Journ. Env. Scis. 2014; 8:39-48.
13. Anjaiah Kumar KL, Vidyasagarachary D. Mapping for artificial recharge sites in Jainoor and Sirpur(U) mandals of Adilabad District, Telangana State, India by electrical resistivity method. Intnatl. Journ. Sci. Res. 2016; 5:386-389.
14. Bandel K, Salameh E. geology development of jordan. Evolution of its rock and life, National Library, Amman, Jordan, 2013; 1:143-215.
15. Quennell AM. Tectonics of the Dead Sea Rift. Proc. Of the 20th Inter, Geol. Conger. Mexico, 1959; 1:385-403.
16. Basem K. The geology of Irbid and Ash Shuna Ash Shamaliyya (Waqqas), NRA, Amman, Jordan, 2000, 3154-II-3154-III.
17. Sawarieh A. Heat sources of the groundwater in the Zara-Zarqa Ma'in-Jiza area, Central Jordan, NRA, Amman, Jordan, 2005; 1:123-147.
18. Natural Resources Authority (NRA) open file, 2000.
19. Ministry of Water and Irrigation (MWI) Open Files, Jordan, 2015. www.mwi.gov.jo.
20. Janardhana Raju N, Reddy TVK, Nayudu PT. Electrical resistivity survey for groundwater in theupper Gunjanaeru Catchment, Cuddapah District, Andhra Pradesh., Jour. Geol. Soc. India. 1996; 47:705-716.
21. Ballukraya PN. Characterizing bounded and weathered/jointed rock aquifers: A case study from Alathur Village, Near Chennai City. Jour. Geol. Soc. India. 2004; 64:784-790.
22. Keller GV, Frischknecht FC. Electrical methods in geophysical prospecting, Pergamon, London, 1966; 1:23-113.
23. Pozdnyakova L, Pozdnyakov A, Zhang R. Application of geophysical methods to evaluate hydrology and soil properties in urban areas Case study. London, UK, 2001; 3:205-216.
24. Bisdorf RJ. Schlumberger soundings at the Amargosa Desert Research Site, Nevada: U.S. Geological Survey Open-File Report. 2002; 140:65.
25. Geological Survey of Canada (GEOSCAN), open file, 2001.
26. Ijeh IB. Investigation of Variation in Resistivity with depth in Parts of Imo River Basin, South-eastern Nigeria. IOSR Journal of Applied Physics (IOSR-JAP). ISSN: 2278-4861. 2014; 6(1):47-54.
27. Frohlich RK, Fisher JJ. Summerly, Electric-hydraulic conductiity correlation in fractured crystalline bedrock: Central Landfill, Rhode Island, USA. J. Applied Geophys. 1996; 35:249-259.
28. Zak I, Freund R. Recent strike slip movement along the Dead Sea Rift. Israel Journal of Earth Sciences. 1966; 15:33-37.
29. Garfunkel Z, Zak I, Freud R. Active faulting in the Dead Sea Rift, Tectononphysics, Elsevier Science Publishers B. V, Amesterdam, 1981; 8:1-26.
30. Klinger Y, Avouac J, Abou Karaki N, Dorbath Bourles D, Reyss L. Slip rate on the Dead Sea transform fault in northern Araba valley (Jordan). Geophs. J. Int. 2000; 2:755-768.